Author Manuscript

Author Manuscript

Author Manuscript

Author Manuscript

HHS Public Access

Author manuscript

Nat Commun. Author manuscript; available in PMC 2012 December 26.

Published in final edited form as:

Nat Commun. ; 3: 724. doi:10.1038/ncomms1727.

Melanoma whole exome sequencing identifies *V600EB-RAF* amplification-mediated acquired B-RAF inhibitor resistance

Hubing Shi[1,8], **Gatien Moriceau**[1,8,*], **Xiangju Kong**[1,8,*], **Mi-Kyung Lee**[1,8,*], **Hane Lee**[2,3,8], **Richard C. Koya**[4,8], **Charles Ng**[5,8], **Thinle Chodon**[5,8], **Richard A. Scolyer**[9,10,12], **Kimberly B. Dahlman**[13,15], **Jeffrey A. Sosman**[14,15], **Richard F. Kefford**[9,11,12], **Georgina V. Long**[9,11,12], **Stanley F. Nelson**[2,3,7,8], **Antoni Ribas**[4,5,6,7,8], and **Roger S. Lo**[1,6,7,8]

[1]Division of Dermatology, Department of Medicine, David Geffen School of Medicine, University of California, LA, California 90095-1662 USA

[2]Department of Human Genetics, David Geffen School of Medicine, University of California, LA, California 90095-1662 USA

[3]Department of Pathology and Laboratory Medicine, David Geffen School of Medicine, University of California, LA, California 90095-1662 USA

[4]Division of Surgical Oncology, Department of Surgery, David Geffen School of Medicine, University of California, LA, California 90095-1662 USA

[5]Division of Hematology & Oncology, Department of Medicine, David Geffen School of Medicine, University of California, LA, California 90095-1662 USA

[6]Department of Molecular and Medical Pharmacology, David Geffen School of Medicine, University of California, LA, California 90095-1662 USA

[7]Jonsson Comprehensive Cancer Center, David Geffen School of Medicine, University of California, LA, California 90095-1662 USA

[8]David Geffen School of Medicine, University of California, LA, California 90095-1662 USA

[9]Melanoma Institute of Australia, University of Sidney, New South Wales, Australia

[10]Royal Prince Alfred Hospital, University of Sidney, New South Wales, Australia

[11]Westmead Millenium Institute, University of Sidney, New South Wales, Australia

Users may view, print, copy, download and text and data- mine the content in such documents, for the purposes of academic research, subject always to the full Conditions of use: http://www.nature.com/authors/editorial_policies/license.html#terms

Address for correspondence: Dr. Roger S. Lo at 52-121 CHS Dept. of Medicine/Dermatology, 10833 Le Conte Ave, Los Angeles, CA 90095-1750 or at rlo@mednet.ucla.edu.

*These authors contributed equally to this work

Author Contributions H.S., G.M., X.K., M-K.L., H.L. designed, performed experiments and analyzed data. R.C.K., C.N., T.C. R.A.S., K.D., J.A.S., R.F.K., G.V.L., A.R., and R.S.L. recruited patient volunteers and/or provided reagents/tissues. H.S., G.M., X.K, M-K.L., H.L., J.A.S., R.F.K., G.V.L., S.F.N. and A.R. contributed to manuscript preparation. R.S.L. designed experiments and research aims, analyzed data, and wrote the paper.

Supplementary Information accompanies this paper at http://www.nature.com/naturecommunications.

Accession codes: Sequence data are archived at the NCBI Sequence Read Archive (SRA) under the accession code SRP010266.

Competing financial interests: A.R. and R.S.L. are the authors of patent application under PCT Application Serial No. PCT/US11/061552 (Compositions and methods for detection and treatment of B-RAF inhibitor-resistant melanomas)

Author Manuscript Author Manuscript Author Manuscript Author Manuscript

[12]University of Sidney, New South Wales, Australia

[13]Department of Cancer Biology, Vanderbilt-Ingram Cancer Center, Nashville, TN 37232

[14]Department of Medicine, Vanderbilt-Ingram Cancer Center, Nashville, TN 37232

[15]Vanderbilt-Ingram Cancer Center, Nashville, TN 37232

Abstract

The development of acquired drug resistance hampers the long-term success of B-RAF inhibitor (B-RAFi) therapy for melanoma patients. Here we show *V600E B-RAF* copy number gain as a mechanism of acquired B-RAFi resistance in four out of twenty (20%) patients treated with B-RAFi. In cell lines, V600E B-RAF over-expression and knockdown conferred B-RAFi resistance and sensitivity, respectively. In *V600E B-RAF* amplification-driven (vs. mutant *N-RAS*-driven) B-RAFi resistance, ERK reactivation is saturable, with higher doses of vemurafenib down-regulating pERK and re-sensitizing melanoma cells to B-RAFi. These two mechanisms of ERK reactivation are sensitive to the MEK1/2 inhibitor AZD6244/selumetinib or its combination with the B-RAFi vemurafenib. In contrast to mutant N-RAS-mediated V600E B-RAF bypass, which is sensitive to C-RAF knockdown, *V600E B-RAF* amplification-mediated resistance functions largely independently of C-RAF. Thus, alternative clinical strategies may potentially overcome distinct modes of ERK reactivation underlying acquired B-RAFi resistance in melanoma.

Introduction

Activating B-RAF V600 kinase mutations occur in ~50% of melanomas[1], and the ATP-competitive type I RAF inhibitors, PLX4032/vemurafenib and GSK2118436, display remarkable activity leading to overall survival advantage in patients with V600B-RAF mutant melanomas[2–6]. Acquisition of drug resistance leading to clinical relapse, however, develops in virtually all patients treated with B-RAF inhibitors (B-RAFi)[4,5]. Heterogeneous mechanisms of acquired B-RAFi resistance hitherto uncovered fall into general MAPK-redundant, AKT-dependent[7,8] or MAPK-reactivating[9,10] pathways, indicating specific translatable therapeutic strategies to prevent or overcome resistance. Contrary to expectation, *V600E B-RAF* secondary mutations have not been found to account for acquired B-RAFi resistance[10], suggesting V600E B-RAF-bypass mechanisms as the principal means to ERK reactivation.

Here we observed an alteration in *V600E B-RAF*, namely genomic copy number gain, in tumors of melanoma patients whose cancer progressed after initial responses to B-RAF inhibitors. We demonstrated that this *V600E B-RAF* amplification results in V600E B-RAF over-expression, which is necessary and sufficient for acquired resistance to B-RAF inhibitor. This finding, along with a recent study reporting N-terminal truncation of V600E B-RAF causing acquired B-RAFi resistance in melanoma[11], underscores key molecular alterations in the drug target itself. We further suggest that V600E B-RAF-instrinsic (amplification, truncation) vs. V600E B-RAF-bypass (N-RAS mutations) mechanisms, both reactivating the MAPK pathway, may offer insights into distinct therapeutic strategies to overcome acquired B-RAFi resistance in melanoma.

Author Manuscript Author Manuscript Author Manuscript Author Manuscript

Results

Whole exome sequencing identifies *V600E B-RAF* amplification

We assembled twenty sets of patient-matched baseline (prior to B-RAFi therapy) and disease progression (DP) (i.e., acquired B-RAFi resistance) melanoma tissues and analyzed them to identify the proposed mechanisms of acquired B-RAFi resistance in melanoma. These reported mechanisms include N-RAS[10] and MEK1[12] mutations, alternative-spliced ^{V600E}B-RAF variants[11], and over-expression of RTKs (PDGFRβ[7,10], IGF1-R[8]) and COT[9] (Tables 1 and Supplementary Table S1; Supplementary Fig. S1). For DP samples negative for these mechanisms and where there was sufficient frozen and patient-matched normal tissues (from patients #4, 5, 8, 14, 16, 17 & 18), we subjected triads of genomic DNAs (gDNAs) from normal, baseline, and DP tissues to whole exome sequencing. In two available data sets, we searched for somatic DP-specific non-synonymous single nucleotide variants (nsSNVs) and small insertion-deletion (indels), which were exceedingly few in number or absent, respectively, using our bioinformatic workflow (Supplementary Tables S2 and S3). We also analyzed for DP-specific copy number variations (CNVs) from the exome sequence data (Supplementary Table S2). This identified *V600E B-RAF* copy number gains in these two patients' DP tissues (2.2 and 12.8 fold in patients #5 and 8, respectively) relative to their respective baseline tissues (Fig. 1a; Table 1). Gain in *V600E B-RAF* copy number was reflected in corresponding increased gene expression at the protein level (Fig. 1b).

V600E B-RAF amplification was validated by gDNA Q-PCR, producing consistent fold increases in DP-specific *V600E B-RAF* copy number gain (relative to baseline) (2.0 and 14 fold increase in patient #5 and 8 respectively) (Fig. 1c). We then expanded the analysis of *V600E B-RAF* amplification to all twenty paired melanoma tissues and detected *V600E B-RAF* copy number gains in DP samples from two additional patients (2.3 and 3 fold for DP2 of patient #9 & DP of patient #13, respectively) (Fig. 1c; Table 1). We note that these copy number fold increases are likely underestimates of the true changes due to non-tumor diploid cell contents and tumor heterogeneity, as most disease progressive tumors occur from stable residual tumors as a result of partial responses seen in the vast majority of patients treated with B-RAF inhibitors. An increase in the mutant *B-RAF* to WT *B-RAF* ratio was also noted in all four cases of DP harboring *B-RAF* copy number gain when compared to their respective baseline tissues (Fig. 1d), consistent with selection for *V600E B-RAF* (vs. the WT *B-RAF* allele) copy number gain during acquisition of B-RAFi resistance. *V600E B-RAF* amplification was largely mutually exclusive with *N-RAS* mutations (no enrichment in *MEK1* exon 3 mutation was detected in DP vs. baseline tumors), RTK over-expression (no *COT* over-expression detected), as well as a novel mechanism involving *V600E B-RAF* alternative splicing[11] (Table 1; Supplementary Fig. S1).

B-RAFi selects for *V600E B-RAF* gain and over-expression

We have derived vemurafenib/PLX4032-resistant (R) sub-lines by providing continuous vemurafenib exposure to seven human melanoma-derived *V600E BRAF*-positive parental (P) cell lines sensitive to vemurafenib-mediated growth inhibition. Four resistant sub-lines, including M229 R5 and M238 R1[7,10], over-expressed PDGFRβ compared to their parental

Author Manuscript Author Manuscript Author Manuscript Author Manuscript

counterpart. One sub-line (M249 R4[10]) gained a mutation in *N-RAS*, and another (M397 R) an alternatively spliced variant of *V600E B-RAF* resulting in in-frame fusion of exons 1 and 11 (Supplementary Fig. S2). As in our tissue analysis, these mechanisms were identified in a mutually exclusive manner. Another vemurafenib-resistant sub-line, M395 R, was derived from a *V600E B-RAF*-homozygous parental line, M395 P (Supplementary Fig. S3a). Compared to M395 P, M395 R harbors increased copy numbers of *V600E B-RAF* gDNA and cDNA, consistent with a dramatic V600E B-RAF protein over-expression (Supplementary Fig. S3b, c, and d). M395 R displays growth highly resistant to vemurafenib treatment (Supplementary Fig. S4a), and titration of M395 R with vemurafenib (1 h) after a 24 h of drug withdrawal revealed pERK levels to be highly resistant to acute V600E B-RAF inhibition (Supplementary Fig. S4b). This pattern of MAPK reactivation was similar to that seen in a mutant N-RAS-driven, vemurafenib-resistant sub-line, M249 R4, and contrasted with that in the RTK-driven vemurafenib-resistant sub-line, M229 R5 (Supplementary Fig. S4b)[7,10]. Expectedly, the levels of p-AKT are unchanged (Fig. 2b) comparing M395 P vs. M395 R, consistent with a lack of RTK over-expression leading to MAPK-redundant, PI3K-AKT signaling[7]. Accordingly, M395 R does not over-express either PDGFRβ or IGF-1R, in contrast to M229 R5, which has been shown to over-express the RTK PDGFRβ (Supplementary Fig. S4c)[7,8]. Additionally, M395 R is WT for N-, H- and K-RAS and MEK1, harbors no secondary mutations in *V600E B-RAF* or an alternatively spliced variant of *V600E B-RAF* which results in a N-terminally truncated V600E B-RAF protein.

Modest *V600E B-RAF* over-expression leads to B-RAFi resistance

Three different but uniformly modest levels of V600E B-RAF over-expression were achieved by infecting M395 P with varying viral titers and subsequent puromycin selection. This resulted in relatively low (1.9 fold over empty vector virus control), medium (2.4 fold) and high (2.8 fold) levels of V600E B-RAF RNA/cDNA over-expression (Supplementary Fig. S5), with the corresponding protein over-expression levels shown in Figure 2a. In comparison, in two sets of tissues (from patients #8 and #13) where flash-frozen tissues were available, the RNA/cDNA levels of V600E B-RAF in the DP tumors were 9.5 and 1.4 fold relative to those in their patient-matched baseline tumors. Notably, the DP tumor from patient #13 was obtained by an intervention radiology-guided needle biopsy of a pelvic mass (Supplementary Table S1) and contained a high admixture of normal and tumor contents (latter indicated by S100), which likely contributed to an underestimation of the true change in the V600E B-RAF RNA/cDNA levels.

V600E B-RAF gain leads to drug-saturable resistance

The modest and incremental over-expression of V600E B-RAF at the RNA and protein levels in M395 P conferred similar degrees of vemurafenib resistance (Fig. 2b). Interestingly, further V600E B-RAF over-expression at a much greater level, as in the case of M395 R relative to M395 P (increase in RNA/cDNA level shown in Supplementary Fig. S3c and S5; increase in protein level shown in Fig. 2c) conferred enhanced drug resistance mainly at 1 μM vemurafenib but not 10 μM vemurafenib (Fig. 2d). Thus, a modest *V600E B-RAF* copy number gain and over-expression can confer vemurafenib resistance, and even high amplitude *V600E B-RAF* amplification and over-expression can be readily saturable by micromolar concentrations of vemurafenib.

Author Manuscript Author Manuscript Author Manuscript Author Manuscript

Moreover, ^{V600E}B-RAF knockdown in M395 R confers vemurafenib sensitivity (Fig. 2c and d). Consistently, ^{V600E}B-RAF over-expression in M395 P (at a level titrated to be comparable to M395 R) and its knockdown in M395 R resulted in pERK resistance and sensitivity, respectively, to acute vemurafenib treatment after a 24 h drug withdrawal (Fig. 2e). We predicted that, regardless of the cellular genetic context, MAPK reactivation due to drug target (i.e., ^{V600E}B-RAF) over-expression would be saturable by higher doses of vemurafenib, in contrast to mutant N-RAS-mediated MAPK reactivation where ^{V600E}B-RAF may be bypassed by the alternative use of C-RAF[13]. Indeed, dosing of vemurafenib from 1 to 50 μM revealed a significant difference in drug sensitivity of M249 R4 (^{Q61K}*N-RAS*) vs. M395 R (amplified ^{V600E}*B-RAF*) (Fig. 3a) (where the latter was highly sensitive to vemurafenib at this drug concentration range), suggesting a potential therapeutic opportunity. To rule out that these results were not due to a difference in genetic backgrounds, we artificially rendered the ^{V600E}*B-RAF* melanoma cell line, M229, vemurafenib-resistant by either ^{Q61K}N-RAS or ^{V600E}B-RAF viral transduction (Fig. 3b). Again, high dose vemurafenib treatment was more effective at overcoming drug resistance in ^{V600E}B-RAF-transduced M229 than in the same cell line transduced with ^{Q61K}N-RAS.

MEK inhibition restores vemurafenib sensitivity

Since both *N-RAS* mutation and ^{V600E}*B-RAF* amplification-driven acquired resistance mechanisms would be anticipated to result in MEK reactivation, we tested the allosteric MEKi, AZD6244/selumetinib, on the ^{Q61K}*N-RAS*-driven M249 R4 and the ^{V600E}*B-RAF* amplification-driven M395 R sub-lines. MEKi treatment resulted in decreased proliferation in both cases, but the activity was noted at lower concentrations for the ^{Q61K}*N-RAS*-driven resistance mechanism (Fig. 3c). This differential pattern was reproducible by exposing AZD6244/selumetinib to ^{V600E}*B-RAF* melanoma cell lines M229 and M238 transduced with high levels of ^{V600E}*B-RAF* vs. a short-term culture, Pt55 R[10], with ^{Q61K}*N-RAS*-driven acquired B-RAFi resistance (Fig. 3d). We also tested the combination of B-RAFi with MEKi, which is currently in clinical testing[14], in three-day survival assays. A calculation of combination index (CI) values using equal ratios of vemurafenib and selumetinib was performed. The results were consistent with a highly synergistic effect of these two agents combined in overcoming both mutant *N-RAS*-driven (M249 R4) and ^{V600E}*B-RAF* amplification-driven B-RAFi resistance (M395 R) (Fig 3e and 3f), although the combination tended to be more potent against mutant N-RAS-driven acquired resistance to vemurafenib. This B-RAFi and MEKi combinatorial synergy was further corroborated in longer-term clonogenic assays (Fig. 3g).

Differential C-RAF dependency of ERK-reactivating mechanisms

We also predicted that MAPK reactivation due to ^{V600E}B-RAF over-expression would be C-RAF-independent, in contrast to mutant N-RAS-mediated MAPK reactivation where ^{V600E}B-RAF may be bypassed by the alternative use of C-RAF. Indeed, C-RAF knockdown by shRNA sensitized the mutant *N-RAS* sub-line, M249 R4, but not the ^{V600E}*B-RAF* amplified sub-line, M395 R, to vemurafenib in three-day survival assays (Fig. 3h). C-RAF knockdown restored vemurafenib sensitivity to M249 R4 (^{Q61K}*N-RAS*/^{V600E}*B-RAF*) even more strikingly in a longer-term clonogenic assays which afforded fresh drug replacement every two days (Fig. 3i). An independent C-RAF shRNA also restored

Author Manuscript Author Manuscript Author Manuscript Author Manuscript

vemurafenib sensitivity to M249 R4 (Supplementary Table S4). Additionally, B-RAFi and MEKi synergy and C-RAF-dependence in mutant N-RAS-driven acquired B-RAFi resistance was confirmed in a short-term culture derived from a tumor with clinical acquired vemurafenib resistance (Supplementary Fig. S6).

Discussion

Identification of ^{V600E}*B-RAF* amplification as a mechanism of acquired resistance in B-RAFi treated patients provides evidence for alterations in the drug target causing clinical relapse. Based on these studies, therapeutic stratification of MAPK reactivation underlying B-RAFi resistance into drug-saturable or C-RAF-dependent pathways may be translatable into the design of next-generation clinical trials aimed at preventing or overcoming B-RAFi resistance (Fig. 4). These findings also provide pre-clinical rationale for dose escalation studies in selected patients with B-RAFi-resistant $^{V600E/K}$*B-RAF* metastatic melanomas, particularly given the wide range of effective dosing and the fact that the maximum tolerated dose of GSK2118436 has not been determined. The combination of current B-RAF inhibitors (or next-generation RAF inhibitors that enhance B-RAF potency or feature pan-RAF inhibition) with MEK1/2 inhibitors may potentially broadly block MAPK reactivation.

Emerging evidence points to *B-RAF* mutant cancers of other tissue origin or lineage being less responsive to specific B-RAF inhibition than *B-RAF* mutant melanomas. Mechanisms of acquired B-RAF inhibitor resistance may turn out to be instructive for understanding primary resistance of *B-RAF* mutant cancer types to B-RAF inhibitors, as primary (de novo) and secondary (or acquired) drug resistance may be clinical manifestations from a spectrum of molecular alterations that are mechanistically linked. Thus, multiple modes (e.g., mutation, copy number gain) of up-regulating oncogene activity, which may pre-exist in the same tumor and/or patient, may help explain the range of heterogeneous responses of *B-RAF* mutant cancers to direct B-RAF, MEK or ERK inhibition.

Methods

Cell culture experiments

Cells were maintained in DMEM with 10 or 20% fetal bovine serum and glutamine. shRNAs (Supplementary Table S4) for *B-RAF* and *C-RAF* were sub-cloned into the lentiviral vector pLL3.7; pBabe B-RAF (V600E) was purchase (plasmid 17544, Addgene); viral supernatants generated by co-transfection with three packaging plasmids into HEK293T cells; and infections carried out with protamine sulfate. Stocks and dilutions of PLX4032 (Plexxikon, Berkeley, CA) and AZD6244 (commercially available) were made in DMSO. Cells were quantified using CellTiter-GLO Luminescence (Promega) or crystal violet staining followed by NIH Image J quantification.

Whole exome sequencing

Human tissues were obtained with patient-informed consent under UCLA Institutional Review Board (#10-001089) approval. For each sample, 3ug of high molecular weight genomic DNA was used as the starting material to generate the sequencing library. Exome captures were performed using Agilent SureSelect Human All Exon 50mb and Agilent

Author Manuscript Author Manuscript Author Manuscript Author Manuscript

SureSelect Human All Exon 50mb XT for PT #5 and Pt #8, respectively, per manufacturers' recommendation, to create a mean 200bp insert library. For Pt #5, sequencing was performed on Illumina GenomeAnalyzerII (GAII) as 76+76bp paired-end run. The normal sample was run on 1 flowcell lane and the tumor samples were run on 2 flowcell lanes each. For Pt #8, sequencing was performed on Illumina HiSeq2000 as 50+50bp paired-end run and 100+100bp paired-end run. The three samples (normal, baseline and DP) were initially mixed with 9 other samples and run across 5 flowcell lanes for the 50+50bp run. For the 100+100bp run, they were mixed with 3 other samples to be run across 5 flowcell lanes with barcoding of each individual genomic sample library.

For Pt #5, approximately 62 million, 137 million, 147 million reads were generated for normal tissue (skin), baseline melanoma and DP melanoma, respectively, with 75.2%, 78.1%, and 74.7% of the reads mapping to capture targets. Based on an analysis of reads that uniquely aligned to the reference genome and for which the potential PCR duplicates were removed, an average coverage of 52X, 88X, and 114X was achieved with 87%, 92% and 93% of the targeted bases being covered at 10X or greater read depth for normal, baseline and DP, respectively.

For Pt #8, approximately 198 million, 270 million, 256 million reads were generated for normal tissue (skin), baseline melanoma and DP melanoma, respectively with 43.2%, 44.1% and 42.3% of the reads mapping to capture targets. Based on an analysis of reads that uniquely aligned to the reference genome and for which the potential PCR duplicates were removed, an average read depth of 107X, 132X and 123X was achieved with 89%, 90% and 90% of the targeted bases being covered at 10X or greater for normal, baseline and DP, respectively.

Sequencing data analysis

For Pt #8 where the samples were indexed and pooled before the sequencing, Novobarcode from Novocraft was used to demultiplex the data. The sequence reads were aligned to the human reference genome using Novoalign V2.07.13 from Novocraft (http://www.novocraft.com). For Pt #5, hg18 downloaded from UCSC genome database was used and for Pt #8, b37 downloaded from GATK (Genome analysis toolkit) resources website was used for the reference genome. SAMtools v.0.1.16[16] was used to sort and merge the data and Picard (http://picard.sourceforge.net/) was used to mark PCR duplicates. To correct the misalignments due to the presence of indels, local realignment was performed using RealignerTargetCreator and IndelRealigner of GATK[17]. Indel calls in dbSNP132 were used as known indel input. Then, GATK CountCovariates and TableRecalibration were used to recalibrate the originally reported quality score by using the position of the nucleotide within the read and the preceding and current nucleotide information. Finally, to call the single nucleotide variants (SNVs), the GATK UnifiedGenotyper was used to the realigned and re-calibrated bam file while GATK IndelGenotyperV2 was used to call small insertion/deletions (Indels). To generate a list of somatic variants for DP tumor, the difference in allele distribution was calculated using one-sided Fisher's exact test using normal sample or the baseline sample. Variants with p-value<0.05 were included in the "somatic variant list". Low coverage (<10X) SNVs and SNVs with more than one variant allele in normal tissue

Author Manuscript Author Manuscript Author Manuscript Author Manuscript

and baseline melanoma were filtered out during the process. These somatic variants were further annotated with SeattleSeqSNPannotation (http://gvs.gs.washington.edu/SeattleSeqAnnotation/). For DP-specific, non-synonymous SNVs that result in missense mutations, we assessed the level of amino acid conservation using PhyloP score (provided in UCSC genome database) where a score > 2 implies high conservation and the nature of amino substitution using Polyphen-2 analysis[18].

CNV analysis was performed using an R package, ExomeCNV[15]. ExomeCNV uses the ratio of read depth between two samples at each capture interval. Here, the read depth data between baseline and DP melanomas were compared. Briefly, the read depth information was extracted through the PILEUP file generated from the BAM file after removing PCR duplicates using SAMtools. The average read depth at each capture interval was calculatedand the classify.eCNV module of ExomeCNV was run with the default parameters to calculate the copy number estimate for each interval. Subsequently, another R package commonly used to segment the copy number intervals, DNAcopy[19], was called through ExomeCNV multi.CNV.analyze module with default parameters to do segmentation and sequential merging. The genomic regions with copy number 1 were called deletion and any regions with copy number >2 were called amplification. Circos[20] was used to visualize the CNV data.

Protein detection

Western blots were probed with antibodies against p-ERK1/2 (T202/Y204), ERK1/2, C-RAF, AKT (Ser473), AKT (Thr308), AKT (Cell Signalig Technologies; all at 1:1000), N-RAS, B-RAF (Santa Cruz Biotechnology; both at 1:500), and tubulin (Sigma; 1:700). For B-RAF immunohistochemistry, paraffin-embedded formalin-fixed tissue sections were antigen-retrieved, incubated with the primary antibody (Santa Cruz Biotechnology; 1:50) followed by HRP-conjugated secondary antibody (Envision System, DakoCytomation). Immunocomplexes were visualized using the DAB (3,3′-diaminobenzidine) peroxidase method and nuclei hematoxylin-counterstained.

Genomic DNA and RNA quantifications

For real-time quantitative PCR, total RNA was extracted and cDNA quantified by the iCycler iQ Real Time PCR Detection System (BioRad). Data were normalized to *TUBULIN* and *GAPDH* levels. Relative expression is calculated using the delta-Ct method. gDNAs were extracted using the FlexiGene DNA Kit (Qiagen) (Human Genomic DNA-Female, Promega). *B-RAF* relative copy number was determined by quantitative PCR (cycle conditions available upon request) using the MyiQ single color Real-Time PCR Detection System (Bio-Rad). Total DNA content was estimated by assaying β-globin for each sample, and 20 ng of gDNA was mixed with the SYBR Green QPCR Master Mix (Bio-Rad) and 2 pmol/L of each primer. All primer sequences are provided in Supplementary Table S4.

Data processing

Statistical analyses were performed using InStat 3 Version 3.0b (GraphPad Software); graphical representations using DeltaGraph or Prism (Red Rock Software); and combination index calculation using CalcuSyn V2.1 (Biosoft). Calculations were made by CalcuSyn

Author Manuscript Author Manuscript Author Manuscript Author Manuscript

software using the method of Chou and Taladay. Interpretation of CI values is summarized as follows: CI < 0.1 (very strong synergy); = 0.1–0.3 (strong synergy); = 0.3–0.7 (synergy); 0.7–0.85 (moderate synergy); = 0.85–0.9 (slight synergy); = 0.90–1.10 (nearly additive); and = 1.10–1.20 (slight antagonism). The relevant correlated Log_{10} (CI) values are shown as follow: Log_{10} (CI 0.1) = −1; Log_{10} (CI 0.3) = −0.5228787452803376; Log_{10} (CI 0.7) = −0.1549019599857432, and Log_{10} (CI 0.85) = −0.07058107428570727.

Supplementary Material

Refer to Web version on PubMed Central for supplementary material.

Acknowledgments

We are grateful to G. Bollag (Plexxikon Inc.) for providing PLX4032, J. S. Economoufor biopsies, N. Doan for immunohistochemistry, B. Chmielowski and J. Glaspy for coordinated patient care, T.L. Toy for technical help with library generation for deep sequencing, and B. Harry for help with analysis of whole exome sequence data. R.S.L. acknowledges funding from the following: Burroughs Wellcome Fund, National Cancer Institute (K22CA151638), V Foundation for Cancer Research, Melanoma Research Foundation, Melanoma Research Alliance, American Skin Association, Joint Center for Translational Medicine, Sidney Kimmel Foundation, Stand Up to Cancer, Eli & Edythe Broad Center of Regenerative Medicine & Stem Cell Research, the Wesley Coyle Memorial Fund, Ian Copeland Melanoma Fund, Ruby Family Foundation, Louis Belley and Richard Schnarr Fund, and The Seaver Institute. R.F.K and G.V.L are supported by Program Grant No. 402761 from the National Health and Medical Research Council of Australia, Translational Research Program Grant No. 05/TPG/1-01 from the Cancer Institute New South Wales (CINSW). J.A.S. is supported by National Cancer Institute (K24CA097588) and American Cancer Society Melanoma Professorship. We are grateful to every patient volunteer who donated tissue(s) for this study.

References

1. Davies H, et al. Mutations of the BRAF gene in human cancer. Nature. 2002; 417:949–954. [PubMed: 12068308]
2. Bollag G, et al. Clinical efficacy of a RAF inhibitor needs broad target blockade in BRAF-mutant melanoma. Nature. 2010; 467:596–599. [PubMed: 20823850]
3. Chapman PB, et al. Improved survival with vemurafenib in melanoma with BRAF V600E mutation. N Engl J Med. 2011; 364:2507–2516. [PubMed: 21639808]
4. Flaherty KT, et al. Inhibition of mutated, activated BRAF in metastatic melanoma. N Engl J Med. 2010; 363:809–819. [PubMed: 20818844]
5. Kefford R, et al. Phase I/II study of GSK2118436, a selective inhibitor of oncogenic mutant BRAF kinase, in patients with metastatic melanoma and other solid tumors. J Clin Oncol. 2010; 28(suppl):abstr 8503.
6. Ribas A, et al. BRIM-2: An open-label, multicenter phase II study of vemurafenib in previously treated patients with BRAF V600E mutation-positive metastatic melanoma. Journal of Clinical Oncology. 2011; 29(suppl):abstr 8509.
7. Shi H, Kong X, Ribas A, Lo RS. Combinatorial treatments that overcome PDGFRβ-driven resistance of melanoma cells to B-RAF(V600E) inhibition. Cancer Research. 2011; 71:5067–5074. [PubMed: 21803746]
8. Villanueva J, et al. Acquired Resistance to BRAF Inhibitors Mediated by a RAF Kinase Switch in Melanoma Can Be Overcome by Cotargeting MEK and IGF-1R/PI3K. Cancer Cell. 2010; 18:683–695. [PubMed: 21156289]
9. Johannessen CM, et al. COT drives resistance to RAF inhibition through MAP kinase pathway reactivation. Nature. 2010; 468:968–972. [PubMed: 21107320]
10. Nazarian R, et al. Melanomas acquire resistance to B-RAF(V600E) inhibition by RTK or N-RAS upregulation. Nature. 2010; 468:973–977. [PubMed: 21107323]

Author Manuscript Author Manuscript Author Manuscript Author Manuscript

11. Poulikakos PI, et al. Acquired resistance to RAF inhibitors is mediated by splicing isoforms of BRAF (V600E) that dimerize in a RAS independent manner. Nature. 2011; 480:387–390. [PubMed: 22113612]
12. Wagle N, et al. Dissecting therapeutic resistance to RAF inhibition in melanoma by tumor genomic profiling. J Clin Oncol. 2011; 29:3085–3096. [PubMed: 21383288]
13. Dumaz N, et al. In melanoma, RAS mutations are accompanied by switching signaling from BRAF to CRAF and disrupted cyclic AMP signaling. Cancer Res. 2006; 66:9483–9491. [PubMed: 17018604]
14. Infante JR, et al. Phase I/II study to assess safety, pharmacokinetics, and efficacy of the oral MEK 1/2 inhibitor GSK1120212 (GSK212) dosed in combination with the oral BRAF inhibitor GSK2118436 (GSK436). Journal of Clinical Oncology. 2011; 29(suppl):abstr CRA8503.
15. Sathirapongsasuti JF, et al. Exome Sequencing-Based Copy-Number Variation and Loss of Heterozygosity Detection: ExomeCNV. Bioinformatics. 2011; 27:2648–2654. [PubMed: 21828086]
16. Li H, et al. The Sequence Alignment/Map format and SAMtools. Bioinformatics. 2009; 25:2078–2079. [PubMed: 19505943]
17. McKenna A, et al. The Genome Analysis Toolkit: a MapReduce framework for analyzing next-generation DNA sequencing data. Genome Res. 2010; 20:1297–1303. [PubMed: 20644199]
18. Adzhubei IA, et al. A method and server for predicting damaging missense mutations. Nat Methods. 2010; 7:248–249. [PubMed: 20354512]
19. Olshen AB, Venkatraman ES, Lucito R, Wigler M. Circular binary segmentation for the analysis of array-based DNA copy number data. Biostatistics. 2004; 5:557–572. [PubMed: 15475419]
20. Krzywinski M, et al. Circos: an information aesthetic for comparative genomics. Genome Res. 2009; 19:1639–1645. [PubMed: 19541911]

Author Manuscript Author Manuscript Author Manuscript Author Manuscript

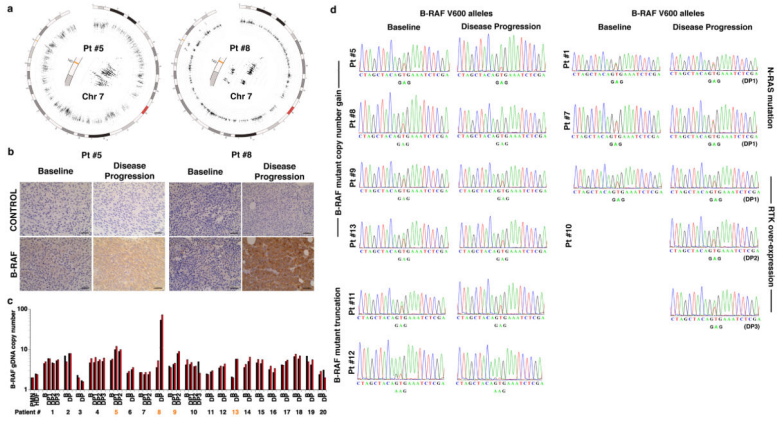

Figure 1. Exome sequencing identifies *^{V600E}B-RAF* amplification as a candidate mechanism for BRAFi resistance

(a) Copy number variations (CNVs) called from whole exome sequence data on two triads of gDNAs using ExomeCNV and chromosome 7 as visualized by Circos (outer ring, genomic coordinates (Mbp); centromere, red; inner ring, log ratio values between baseline and disease progression (DP) samples' average read depth per each capture interval; scale of axis for Pt #5 −5 to 5 and for Pt #8 −2.5 to 2.5). Two patients whose melanoma responded to and then progressed on vemurafenib. The genomic region coded orange represents the location of B-RAF (chr7:140,424,943–140,524,564), which shows an average log ratio value of 1.14 (2.2 fold gain; Pt #5) and 3.8 (12.8 fold gain; Pt #8). **(b)** B-RAF immunohistochemistry on paired tissues derived from the same patients as in a (scale bar = 50 μM) **(c)** Validation of *^{V600E}B-RAF* copy number gain by gDNA qPCR (black and red by B-RAF primer set 1 and 2, respectively) and recurrence across distinct patients (positives highlighted in orange). PMN, peripheral mononuclear cells, and HDF, human dermal fibroblasts for diploid gDNAs. **(d)** *B-RAF* V600 mutant to WT ratio increases with disease progression or acquisition of B-RAFi resistance mediated by mutant *B-RAF* copy number gain. Chromatograms from Sanger sequencing for melanoma samples from patients who acquired B-RAFi resistance based on distinct molecular alterations: *^{V600E}B-RAF* copy number gain, *^{V600E}B-RAF* truncation, *N-RAS* mutation or RTK over-expression.

Author Manuscript Author Manuscript Author Manuscript Author Manuscript

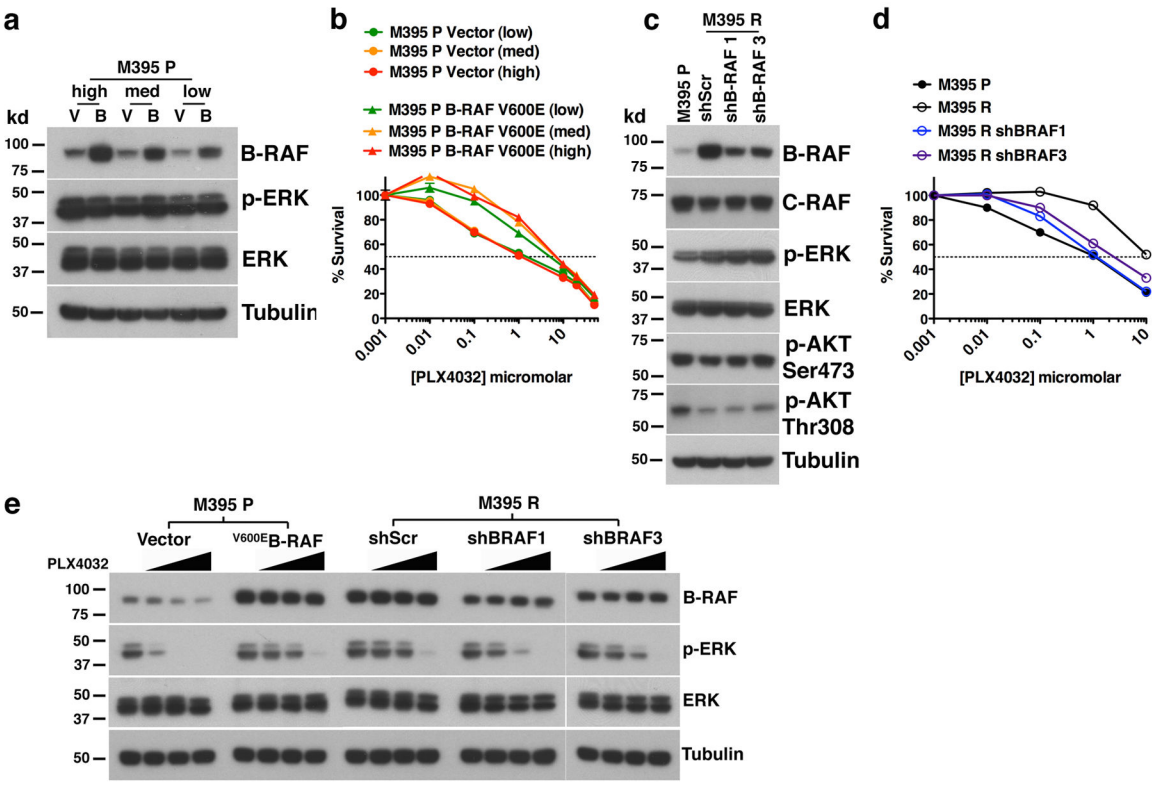

Figure 2. ^{V600E}B-RAF levels modulate melanoma sensitivity to vemurafenib

(a, b) Western blot of ^{V600E}B-RAF^{V600E} and p-ERK, tubulin is used as a loading control. Growth curve of did not alter the pERK level in the absence of vemurafenib/PLX4032 but conferred growth resistance to the parental line, M395 P when exposed to indicated concentrations of PLX4032 for 72 h (relative to DMSO-treated controls; mean ± SEM, n = 5). Dashed line, 50% inhibition. **(c, d)** Transduction of shRNA to knockdown BRAF^{V600E} in the drug-resistant sub-line, M395 R, did not alter the pERK level in the absence of PLX4032 but restored growth sensitivity to PLX4032 (72 h; mean ± SEM, n = 5). **(e)** Increasing (in M395 P) or decreasing (in M395 R) BRAF^{V600E} levels decreased or increased pERK sensitivity to PLX4032 (0, 0.1, 1, 10 μM) treatments for 1 h, respectively.

Author Manuscript Author Manuscript Author Manuscript Author Manuscript

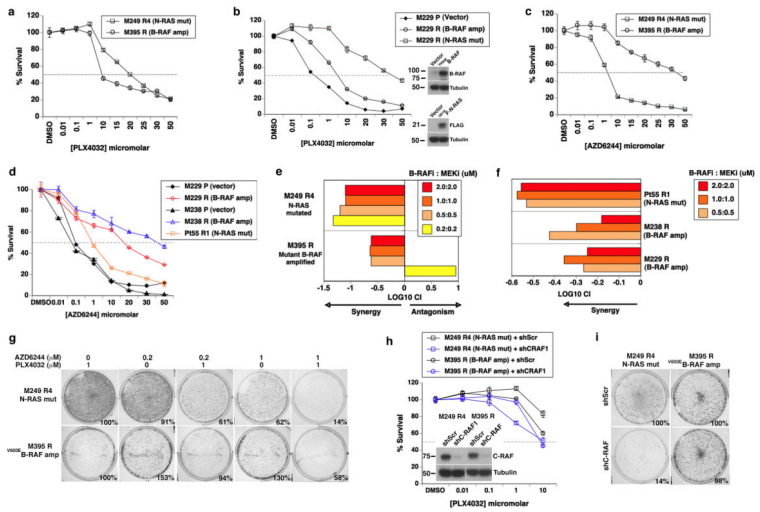

Figure 3. Differential B-RAFi/MEKi sensitivities and C-RAF dependency

(a) Survival curves of B-RAFi acquired resistant sub-lines, with indicated mechanisms of resistance, to 72 h of B-RAFi (PLX4032) treatments, showcasing differential responses at the micro-molar drug range. Results are shown relative to DMSO-treated controls (mean ± SEM, n = 5; dashed line, 50% inhibition). **(b)** Survival curves of cell lines, engineered by viral transduction of M229 P to be B-RAFi resistant, to 72 h of B-RAFi (PLX4032) treatments, showcasing differential responses at the micro-molar drug range. Results are shown relative to DMSO-treated controls (mean ± SEM, n = 5). Expression of indicated viral expression constructs shown in Western blots. (**c**) Survival curves of B-RAFi acquired resistant sub-lines, with indicated mechanisms of resistance, to 72 h of MEKi (AZD6244) treatments, showcasing differential responses at the micro-molar drug range. Results are shown relative to DMSO-treated controls (mean ± SEM, n = 5). (**d**) Survival curves of cell lines (engineered by viral transduction of M229 P and M238 P to over-express ^{V600E}B-RAF rendering these parental cells resistant to B-RAFi) to 72 h of MEKi (AZD6244) treatments, showcasing differential responses at the micro-molar drug range. Pt55 R (double *B-RAF* and *N-RAS* mutant) is a short-term melanoma culture derived from a tumor which acquired PLX4032 (vemurafenib) resistance in a treated patient. Results are shown relative to DMSO-treated controls (mean ± SEM, n = 5). **(e** and **f)** Indicated cell lines were treated with constant ratios of PLX4032 and AZD6244 and survival measured after 72h. Relative synergies, expressed as $\log_{10}$ of CI values, are shown. **(g)** M249 (R4) and M395 R were seeded at single cell density and treated with indicated concentrations of PLX4032 and/or AZD6244. Inhibitors and media were replenished every two days, colonies visualized by crystal violet staining after 8 days of drug treatments, and quantified (% growth relative to cells treated with 1 μM PLX4032; representative of 2 experiments). Photographs representative of two independent experiments. **(h)** Survival curves of indicated cell lines after shScrambled or shC-RAF transduction (inset) and when treated with PLX4032 for 72 h. **(i)** Clonogenic assays of cell lines in e with 14 days (M249 R4) or 18 days (M395 R) of PLX4032 treatment. Results are representative of 2 experiments.

Author Manuscript Author Manuscript Author Manuscript Author Manuscript

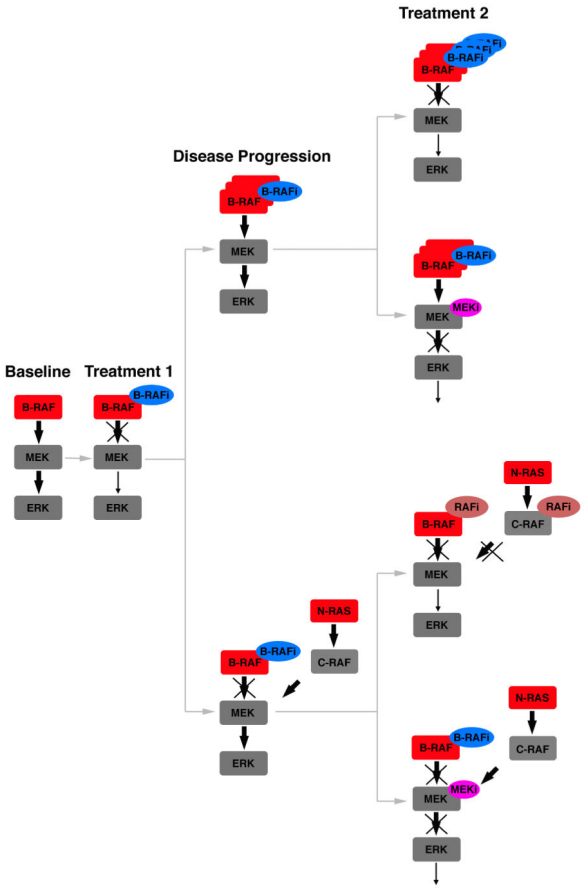

Figure 4. MAPK-reactivating mechanisms of acquired B-RAFi resistance and therapeutic implications

Distinct strategies to overcome acquired resistance driven by amplification of mutant *B-RAF* or mutations in *N-RAS*. Schematic of ERK-reactivating pathways (^{V600E}*B-RAF* amplification indicated by stacked symbols, top; *N-RAS* mutation, bottom; mutant proteins in red and WT proteins in grey) and proposed strategies to restore B-RAFi sensitivity (increasing B-RAFi concentration or potency, top; switching B-RAFi to pan-RAFi, bottom). Alternatively, the combination of B-RAFi and MEKi are predicted to synergistically growth-inhibit melanomas with acquired resistance to B-RAFi monotherapy stemming from ERK reactivation.

Author Manuscript Author Manuscript Author Manuscript Author Manuscript

Table 1

Clinical characteristics and acquired resistance mechanisms in patients with matched baseline and disease progression (DP) melanomas tissues.

Study Site	Pt #	Age & Gender	Stage	RECIST 1.1 best overall response	PFS (days)	Biopsies	Relative B-RAF CN gain*	B-RAF Truncation In DP**	N-RAS mutation in DP***	RTK in DP****	MEK1 mutation in DP*****
UCLA	1	65F	M1c	−37%	279	B					
						DP1			+		
						DP2			+		
						DP3					
	2	30M	M1b	−14%	113	B					
						DP		N/A		+	
	3	46M	M1c	−32%	149	B					
						DP		N/A		N/A	
	4	66F	M1b	−53%	137	B					
						DP1					
						DP2					
						DP3					
	5	48M	M1c	−24%	126	B					
						DP1	+				
						DP2	+				
	6	54M	M1c	−75%	84	B					
						DP		N/A		+	
	7	65F	M1c	−72%	373	B					
						DP1			+		
						DP2			+		
	8	51M	M1c	−60%	212	B					
						DP	+				
	9	47F	M1b	−72%	97	B					
						DP1		N/A		N/A	
						DP2	+	N/A	+	N/A	

Author Manuscript Author Manuscript Author Manuscript Author Manuscript

Study Site	Pt #	Age & Gender	Stage	RECIST 1.1 best overall response	PFS (days)	Biopsies	Relative B-RAF CN gain*	B-RAF Truncation In DP**	N-RAS mutation in DP***	RTK in DP****	MEK1 mutation in DP*****
	10#	47F	IIIc	−31%	238	B					
						DP1				+	
						DP2				+	
						DP3				+	
	11	52M	M1c	−70%	104	B					
						DP		+			
	12	65M	M1c	−22%	161	B					
						DP		+			
	13	60F	M1a	−42%	133	B					
						DP	+				
MIA	14#	59M	M1c	−14%	224	B					
						DP					
	15	71M	M1c	−53%	239	B					
						DP		N/A	+	N/A	
	16#	38F	M1a	−100%	119	B					
						DP		N/A		N/A	
	17#	39M	M1c	−56%	118	B					
						DP		N/A		N/A	
	18#	58F	M1c	−63%	209	B					
						DP					
VI	19	46F	M1c	−59%	107	B					
						DP		N/A		N/A	
	20	70F	M1a	−70%	183	B					
						DP			+	N/A	

UCLA, University of California, Los Angeles; MIA, Melanoma Institute, Australia; VI, Vanderbilt-Ingram Cancer Center

Patient numbers followed by the # symbol denote those patients treated with the B-RAFi, dabrafenib/GSK2118436. All other patients were treated with the B-RAFi vemurafenib/PLX4032.

Patient numbers 1, 4, 5, 7, 8, 10, 11, 12 and 20 correspond to patient numbers 16, 7, 15, 10, 9, 8, 5, 6, and 2, respectively, in Poulikakos et al, Nature (2011) 480:387–390[11].

Author Manuscript Author Manuscript Author Manuscript Author Manuscript

Patient numbers 1, 2, 3, 4, 5, 6 and 19 correspond to patients 55, 48, 92, 111-001, 111-010, 104-004, and 56 in Nazarian et al, Nature (2010) 468:973–977.

DP samples are scored positive (+) only when compared to the patient-matched baseline tumors (e.g., a mutation detected in the DP but not in baseline tumor). For clarity, DP samples which scored negative are denoted by empty boxes. N/A, tissues for indicated assays not available.

* See Fig 1c.

** No B-RAF secondary mutations were detected. Truncated B-RAF was detected by Q-PCR (Supplementary Table S4).

*** H-RAS and K-RAS are WT in all DP samples.

**** IHC data presented in Nazarian et al (Nature, 468:973–977, 2010)[10] for Pt #2 and #6. Q-PCR data for other available paired RNA samples shown in Supplementary Fig. S1.

***** Only Exon 3 of MEK1 was sequenced. No MEK1 exon 3 mutation was detected in any DP sample that was not pre-existing in the baseline, pre-treatment sample.

Nat Commun. Author manuscript; available in PMC 2012 December 26.